Triple Point on the Melting Curve and Polymorphism of Nitrogen at High Pressure

Alexander F. Goncharov,[1] Jonathan C. Crowhurst,[2] Viktor V. Struzhkin,[1] and Russell J. Hemley[1]
[1]Geophysical Laboratory, Carnegie Institution of Washington, 5251 Broad Branch Road NW, Washington, D.C. 20015, USA
[2]Lawrence Livermore National Laboratory, University of California, 7000 East Avenue, Livermore, California 94551, USA

(Received 27 March 2008; published 26 August 2008)

Raman spectra of solid and fluid nitrogen to pressures up to 120 GPa and temperatures up to 2500 K reveal that the melting line exhibits a maximum near 70 GPa, followed by a triple point near 87 GPa, after which the melting temperature rises again. Fluid nitrogen remains molecular over the entire pressure range studied, and there is no sign of a fluid-fluid transition. Solid phases obtained on quenching from the melt above 48 GPa are identical to the recently discovered ι and ζ' phases. We find that kinetics plays a major role in the experimentally observed phase changes and account for the metastability of various crystalline molecular phases and the existence of an amorphous single bonded $\eta - \mathrm{N}$.

DOI: 10.1103/PhysRevLett.101.095502 PACS numbers: 62.50.−p, 64.70.D−, 64.70.Ja, 78.30.−j

As an archetypal diatomic system, nitrogen is an excellent testbed for refining models of physical and chemical processes that occur under extreme pressures (P) and temperatures (T). However, static diamond anvil cell (DAC) experiments on nitrogen [1–8] have not yet explored the $P-T$ conditions near the melting line ($>$ 20 GPa) and in the regime approaching polymerization inferred from theoretical calculations [9] and shock-wave experiments (see [10] and references therein). The $P-T$ conditions of synthesis of the polymeric *cubic gauche* nitrogen, cg-N [6,9] are estimated to be $P > 110$ GPa and $T > 2000$ K. Nevertheless, *in situ* phase identification at high P and T has not been reported. It has been suggested that at 120 GPa, the melting temperature of molecular nitrogen is around 2000 K based on visual observations [6]. Recently, similar observations were used to determine the melting line of nitrogen to 71 GPa; a sharp maximum at 50 GPa was interpreted as due to a fluid molecular to fluid polymeric phase transition [11]. Here we report *in situ* Raman measurements in the laser-heated DAC that extend the melting line up to 120 GPa. The results show that nitrogen remains in a diatomic molecular form under these conditions. The melting line flattens above 50 GPa and shows nonmonotonic behavior due to a triple point at 87 GPa and 1550 K. These results provide an explanation for the amorphization of nitrogen at low and moderate temperatures above 120 GPa [2–4].

A variety of heating and Raman techniques were used in this work. Raman (laser heating) with continuous wave (CW) probe (heating) [12,13] was performed to 86 GPa. A thin Ir plate with a central hole was used to absorb incident laser light and thus heat the sample [12–14]. Thin alumina plates, or alternatively alumina deposited directly on to the anvils, ensured adequate thermal insulation. Pulsed laser heating in combination with a pulsed Raman system [15] was used for experiments in the 50–120 GPa pressure range and at temperatures of up to 2500 K. The heating pulses (from an electrically modulated fiber laser) were approximately 2 μs long with a repetition rate of 10 kHz. The Raman probe laser (wavelength 532 nm and pulse length 25 ns) and a gated intensified CCD detector (operating with a corresponding gate width) were synchronized with the heating laser. The sample temperature was highest 10–20 μs after the arrival of the heating laser pulse, so the Raman measurements were performed in the corresponding time window. For both CW and pulsed heating experiments, the total accumulation time normally did not exceed 10 s; during this time the sample temperature was stable based on the repetitive Raman and pyrometric measurements of the coupler temperature before and after Raman spectra collection. More than 30 experiments were performed.

Temperature gradients in the laser heated DAC are typically large (e.g., [16]), and radiometric measurements of thermal emission emitted by the coupler are often expected to differ significantly from the temperature of the actual sample (e.g., [17]). Temperature measurements based on observations of physical properties of the sample itself are potentially more reliable. In the pressure range below approximately 50 GPa in CW laser heating experiments, temperature was determined from the relative intensity of the Raman sidebands corresponding to vibrational transitions (vibrons) from thermally excited levels [14] and from the ratio of anti-Stokes to Stokes peaks (e.g., [18]). At higher pressures, the latter method becomes more useful because of pressure-induced broadening of the vibron bands (including the sidebands). All pressures reported here refer to ruby fluorescence measurements performed before and after heating (which did not differ by more than 1 GPa).

We studied that pressure range where a number of orientationally ordered molecular phases were found to be stable (or metastable) at room temperature (17–120 GPa), namely ε, ζ, and κ (e.g., [7]). Before performing a heating cycle, we always preheated the sample (to approximately 1000 K when thermal radiation becomes visible) to relax the stresses that are built up during the compression at room temperature. This normally results in narrowing of the Raman bands recorded at room temperature. Below 48 GPa initial room temperature phases were recovered after cooling from the highest temperatures. Above 48 GPa, laser heating above the melting line results in the transformation upon cooling to another molecular phase identified as ι nitrogen (N_2) [5] based on the Raman spectrum. Above approximately 70 GPa, yet another molecular phase appears after quenching, but traces of $\iota - N_2$ could be observed up to 114 GPa. The Raman spectra of this high-pressure phase correspond to those reported in Ref. [4] for $\zeta' - N_2$—the product of the back transformation at high temperature from the amorphous polymeric phase, η [2,3].

In situ high-temperature measurements (Fig. 1) show a phase transformation to $\delta - N_2$, which is partially orientationally disordered. This transition was traced in resistive heating Raman experiments to 34 GPa [5]. At the transition [Fig. 1(a)], the ν_2 vibron splitting disappears and the ν_1 vibron (ν_2 and ν_1 correspond to molecules, which occupy sites with different symmetries, e.g. [19]) becomes strongly temperature dependent, both characteristic of $\delta - N_2$ [19]. In some experiments we also observed a change in the low-frequency phonon spectra at the transition: complex multiline spectra of orientationally ordered phases transform to a single broad band of $\delta - N_2$ [Fig. 1(c)]. Using these features, we traced the presence of $\delta - N_2$ to 83 GPa (Fig. 2). At higher pressure, heating of $\zeta' - N_2$ causes a frequency increase and a broadening of the ν_2 vibron band [Fig. 1(b)] due to transformation to $\varepsilon - N_2$ [5] (ν_1 vibron band becomes weak under these conditions [2]). Heating of $\iota - N_2$ results in the same transformation, so there is no need to differentiate the melting behavior discussed below.

Below 83 GPa melting of nitrogen can be detected by observing a red shift of the ν_2 vibron [Fig. 1(a)] and a disappearance of the ν_1 vibron. Coexistence of the solid $\delta - N_2$ and a molecular fluid is clear from the Raman spectra [Fig. 1(a)] and is due to temperature gradients in the sample cavity. The temperatures of solid and fluid

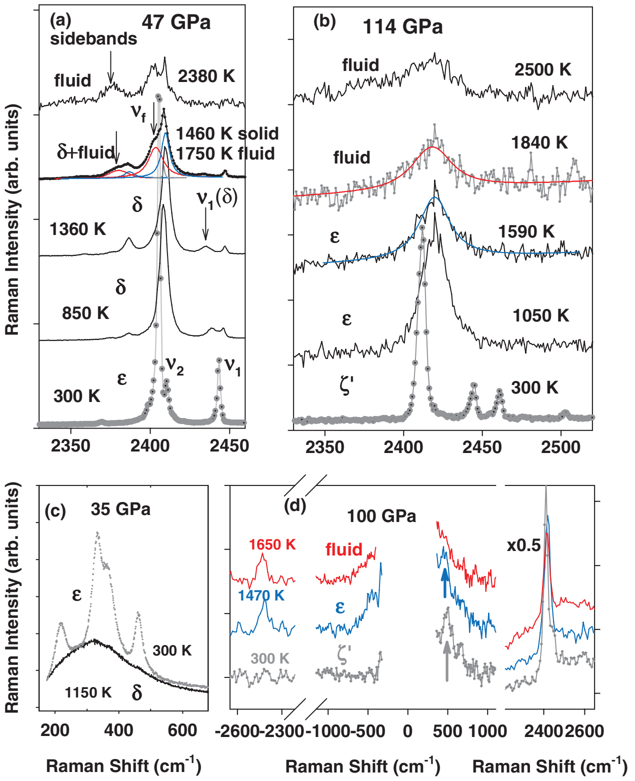

FIG. 1 (color). Raman spectra of laser-heated nitrogen at high static pressures. Arrows indicate the Raman peaks which were used for the phase and melting diagnostics (see text). (a) and (b) vibron Stokes spectra. (c) low-frequency, and (d) the entire spectra. The deconvolution of a Raman spectrum at 47 GPa and 1550 K is shown in (a) to illustrate the spectral components that are involved in the melting and temperature determinations. Combined uncertainties in determination of the band integrated areas is approximately 30%, which propagates to 6% uncertainty in temperature. Single peak fits to the vibron bands are shown in (c) to illustrate the broadening at the melting (FWHM = 23 and 30 cm^{-1} for 1590 and 1840 K curves, respectively). Red lines—fluid, blue lines—solid.

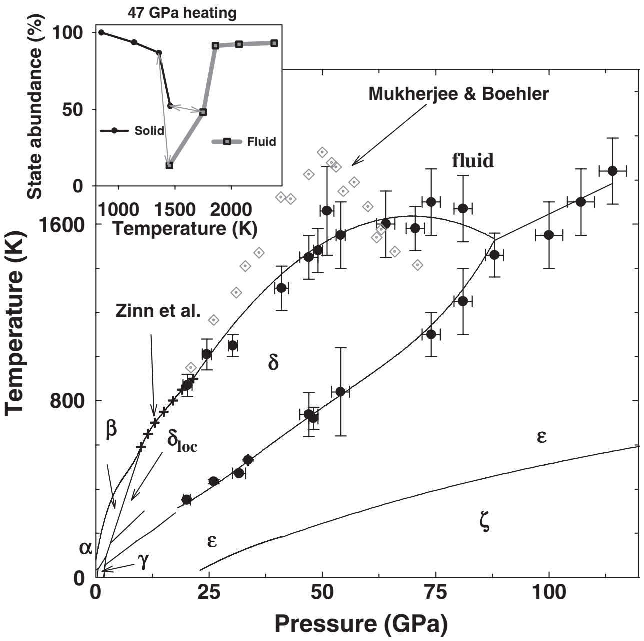

FIG. 2. Phase diagram of nitrogen. Solid symbols indicate data obtained in the present work. Temperature error bars correspond to the propagated errors in the Raman peak intensity determination (Fig. 1) and the temperature probe intervals. Pressure error bars are the estimated largest uncertainties related to pressure measurements at room temperature and pressure drift during heating. Diamonds are the melting data reported in Ref. [11], crosses are the melting data reported in Ref. [1]. The inset shows the relative abundance of solid and fluid phases determined from the relative intensities of the corresponding Raman vibron peaks in Fig. 1(a). Temperatures were determined from the relative intensities of the sidebands. Arrows connect points determined in the same measurement.

components determined from the intensity of the Raman sidebands were within 200 K when thermal insulation was employed, implying measured melting temperatures of corresponding uncertainties (we determined the melting temperature by averaging the highest obtained in the solid state and the lowest in the fluid state). Above 83 GPa melting is indicated by a disappearance of lower frequency phonon modes [Fig. 1(d)] and broadening of the ν_2 vibron [Fig. 1(b)].

The melting line determined here (Fig. 2) agrees well with that obtained in lower-pressure resistive heating experiments [1]. The results below 50 GPa presented here include observations from Ref. [12]. Here we performed a more rigorous analysis of the data, which included consideration of the splitting of the vibron bands and sidebands due to melting; this shifted the melting line to higher temperatures. Our data below 50 GPa after correction are lower than those reported in Ref. [11]. This inconsistency is most likely due to the difference in temperature measurement techniques (the method of Ref. [11] yields the surface temperature of the coupler, which is higher than the bulk of the sample [17]). Also, unlike Ref. [11], we did not observe a sharp maximum at the melting line at 50 GPa. Instead, we observe a slow turnover and a broad maximum near 70 GPa. It should be noted that the beginning of the decline of the melting line in the experiment of [11] coincides with the observations of formation of $\iota - N_2$ in the quenched sample. We suggest that melting and formation of $\iota - N_2$ could be confused in the experiment reported in Ref. [11] since exclusively visual diagnostics were performed (see also Ref. [20]), while the corresponding temperatures may have been overestimated (see above). In contrast our *in situ* Raman measurements provide fingerprints of the material′s state. Our Raman spectra of the quenched sample show coexistence of ι and ε (ζ' at higher pressures) N_2 in the quenched sample and the visual observations are quite similar to those reported in Ref. [11]. Our melting line (Fig. 2) indicates a triple point near 88 GPa. At higher pressures we could not observe characteristic features of $\delta - N_2$. The data thus support the existence of a triple point between fluid, δ-, and $\varepsilon - N_2$ at 88 GPa and 1550 K.

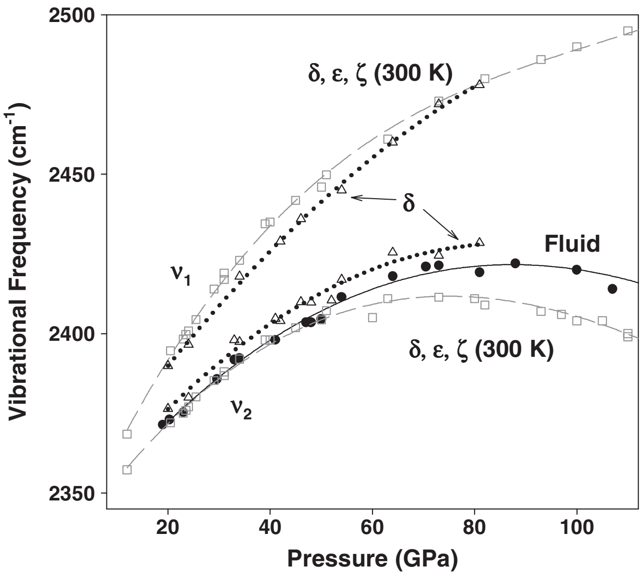

FIG. 3. Pressure dependence of the frequencies of the Raman-active vibrons of solid and fluid phases of nitrogen.

The frequency of the Raman-active vibron of fluid nitrogen shows a turnover and a shallow maximum near 80 GPa (Fig. 3). We find this mode to be only weakly temperature dependent to 2500 K. The solid ε, ζ, κ phases at room temperature show a similar pressure dependence of the ν_1 and ν_2 vibrons. Raman frequencies of $\delta - N_2$ near the melting are between those of the ν_1 and ν_2 vibrons at room temperature (Fig. 3). Naturally, the difference in the ν_1 frequency for δ and $\varepsilon(\zeta) - N_2$ vanishes near the triple point.

The presence of a maximum at the melting line indicates that fluid nitrogen becomes denser than solid $\delta - N_2$ in the pressure range between the maximum and the triple point. This could suggest the existence of a fluid-fluid transformation [11,21]. However, the continuity of our Raman

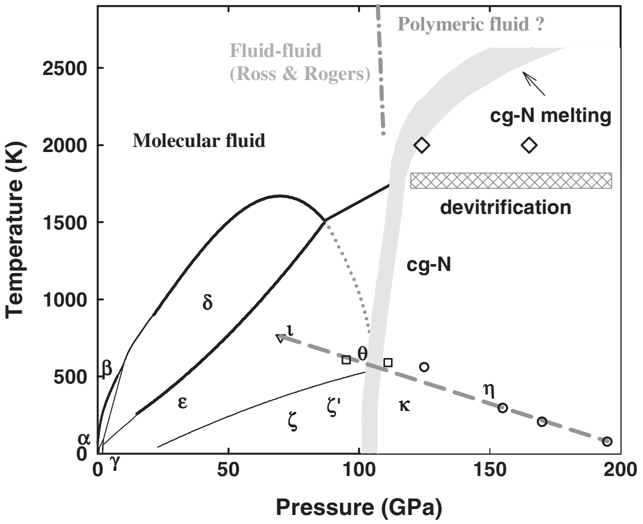

FIG. 4. Proposed high $P - T$ phase diagram of nitrogen. Thin black solid lines determined previously; thick black solid lines: phase boundaries determined in this work. Dashed gray line—kinetic boundary between ε, ζ,κ and ι, θ, η phases, Refs. [3–5], triangle—transitions to ι, squares to θ, circles to η phases. Dotted gray line—metastable extrapolation of the melting line. Light gray area—proposed phase boundary of cg-N (see text) and melting line of cg-N (no data are available). For determination of the slope of the cg-N phase line we used the equations of state [6,7,22,23] and estimations of the vibrational entropy from Refs. [2,6–8,24]. Dash-dotted gray line—the fluid-fluid transition proposed in Ref. [10]. At high temperature it passes through 7000 K at 90 GPa (not shown) according to shock-wave experiments. Black open diamonds—the $P - T$ points where polymeric cg-N was synthesized [6–8].

spectra in the fluid phase provides no evidence for such a transition. Moreover, judging from the presence of the high-frequency vibron band (Fig. 3) due to the N_2 triple bond, fluid nitrogen remains essentially molecular in the pressure range studied. However, if fluid nitrogen near the maximum at the melting line is a two-component system [21], the changes in the Raman spectra may be too subtle to be observed.

A negative slope of the melting line in the pressure range of 66–87 GPa suggests the possibility of pressure-induced amorphization at higher pressures and low temperatures as seen in numerous other materials (H_2O, SiO_2). Indeed, the amorphous single bonded nitrogen, η [2–4] occurs at pressures above the metastable extrapolation of the melting line (Fig. 4) [7,8]. We find that this kinetic boundary is within the stability range of cg-N which we determine by estimating the slope of the equilibrium phase line between molecular (ε and ζ) and polymeric (cg-N) phases and using the results of this work and the previously reported synthesis conditions of cg-N [6–8] as constraints (Fig. 4). The results clearly show that $\eta - N$ is a metastable non-equilibrium state; it transforms to thermodynamically stable cg-N when heated above a corresponding devitrification temperature (Fig. 4) [6–8].

A number of molecular phases has been observed here and previously [5,6] in the pressure range of 50–120 GPa and elevated temperatures. The data of this work show that the ζ-phase (also κ and η phases, which appear on further compression) can only be accessed at $T < 600$ K from $\varepsilon - N_2$. If cooling down after heating to higher temperature or on decompression, these phases never appear; we therefore suggest they are metastable (see also [5]). Using the same criterion, $\varepsilon - N_2$ is only thermodynamically stable near the $\varepsilon - \delta$ phase line. It transforms to $\iota-$ and $\theta - N_2$ along a kinetic boundary that interestingly lies on the extrapolation of the $\kappa - \eta$ kinetic line to lower pressure. The results of this work show that $\iota - N_2$ can be formed at pressure as low as 48 GPa. It can also be obtained by unloading $\theta - N_2$ at 840 K [5]. Thus, we suggest that the ι- phase has a domain of stability in the $P - T$ phase diagram. Using the same criterion, $\zeta' - N_2$ should also have a stability domain: it can be obtained by cooling from the fluid state at 70–120 GPa or by back transformation from $\eta - N$ on pressure decrease. This complex polymorphism shows that several molecular phases have very similar enthalpies, so kinetics plays a major role in the experimentally observed phase changes. The kinetic line suggested here (see also Ref. [20]) between the phases of the ε class (ε, ζ, κ) and other phases (ι, θ, η) indicates the presence of kinetic barriers related to substantial differences in their structures.

In conclusion, Raman measurements combined with laser-heated DAC techniques provide a self-consistent picture of the phase diagram of nitrogen to 120 GPa and 2500 K. Measurements of the melting line and the vibrational properties of fluid nitrogen to these conditions reveal a triple point between two solid molecular and fluid phases at 87 GPa and 1550 K. The melting line has a negative slope prior to the triple point, and thereafter becomes positive. The sharp maximum in the melting line reported in Ref. [11] at 50 GPa is most likely related to the presence of other stable or metastable molecular phases above this pressure.

The authors are grateful to E. Gregoryanz, V. V. Brazhkin, J. A. Montoya, and P.-E. Janolin for discussions. We acknowledge support by DOE/BES, DOE/NNSA (CDAC), and NSF-DMR. This work was performed under the auspices of the U.S. Department of Energy by Lawrence Livermore National Laboratory in part under Contract No. W-7405-Eng-48 and in part under Contract No. DE-AC52-07NA27344.

[1] S. Zinn, D. Schiferl, and M. F. Nicol, J. Chem. Phys. **87**, 1267 (1987); D. A. Young *et al.*, Phys. Rev. B **35**, 5353 (1987).
[2] A. F. Goncharov *et al.*, Phys. Rev. Lett. **85**, 1262 (2000).
[3] M. Eremets *et al.*, Nature (London) **411**, 170 (2001).
[4] E. Gregoryanz *et al.*, Phys. Rev. B **64**, 052103 (2001).
[5] E. Gregoryanz *et al.*, Phys. Rev. B **66**, 224108 (2002).
[6] M. I. Eremets *et al.*, Nature Mater. **3**, 558 (2004).
[7] E. Gregoryanz *et al.*, J. Chem. Phys. **126**, 184505 (2007).
[8] M. J. Lipp *et al.*, Phys. Rev. B **76**, 014113 (2007).
[9] C. Mailhiot, L. H. Yang, and A. K. McMahan, Phys. Rev. B **46**, 14 419 (1992).
[10] M. Ross and F. Rogers, Phys. Rev. B **74**, 024103 (2006).
[11] G. D. Mukherjee and R. Boehler, Phys. Rev. Lett. **99**, 225701 (2007).
[12] A. F. Goncharov and J. C. Crowhurst, J. Low Temp. Phys. **139**, 727 (2005).
[13] J. F. Lin *et al.*, Rev. Sci. Instrum. **75**, 3302 (2004).
[14] A. F. Goncharov and J. C. Crowhurst, Phys. Rev. Lett. **96**, 055504 (2006).
[15] A. F. Goncharov and J. C. Crowhurst, Rev. Sci. Instrum. **76**, 063905 (2005).
[16] B. Kiefer and T. S. Duffy, J. Appl. Phys. **97**, 114902 (2005).
[17] M. Santoro, J.-F. Lin, H.-K. Mao, and R. J. Hemley, J. Chem. Phys. **121**, 2780 (2004).
[18] A. Compaan, H. W. Lo, M. C. Lee, and A. Aydinli, Phys. Rev. B **26**, 1079 (1982).
[19] M. I. M. Scheerboom and J. A. Schouten, Phys. Rev. Lett. **71**, 2252 (1993).
[20] E. Gregoryanz and A. F. Goncharov (private communication).
[21] E. Rapoport, J. Chem. Phys. **46**, 2891 (1967).
[22] R. L. Mills, B. Olinger, and D. T. Cromer, J. Chem. Phys. **84**, 2837 (1986).
[23] H. Olijnyk, J. Chem. Phys. **93**, 8968 (1990).
[24] R. Caracas, J. Chem. Phys. **127**, 144510 (2007).